Supporting Information

Double-layer Graphene Outperforming Monolayer as Catalyst on Silicon Photocathode for Hydrogen Production

Uk Sim[1‡], Joonhee Moon[2,4‡], Joohee Lee[1], Junghyun An[1], Hyo-Yong Ahn[1], Dong Jin Kim[3], Insu Jo[2], Cheolho Jeon[4], Seungwu Han[1], Byung Hee Hong[2,3] and Ki Tae Nam[1*]*

[1]Department of Materials Science and Engineering, Seoul National University, Seoul, Republic of Korea

[2]Department of Chemistry, Seoul National University, Seoul, Republic of Korea

[3]Department of Nano Science and Technology, Graduate School of Convergence Science and Technology, Seoul National University, Seoul, Republic of Korea

[4]Korea Basic Science Institute, Gwahangno, Yusung-gu, Daejeon, 305-333, Korea

Corresponding author

Prof. Byung Hee Hong

E-mail: byunghee@snu.ac.kr

Prof. Ki Tae Nam

E-mail: nkitae@snu.ac.kr

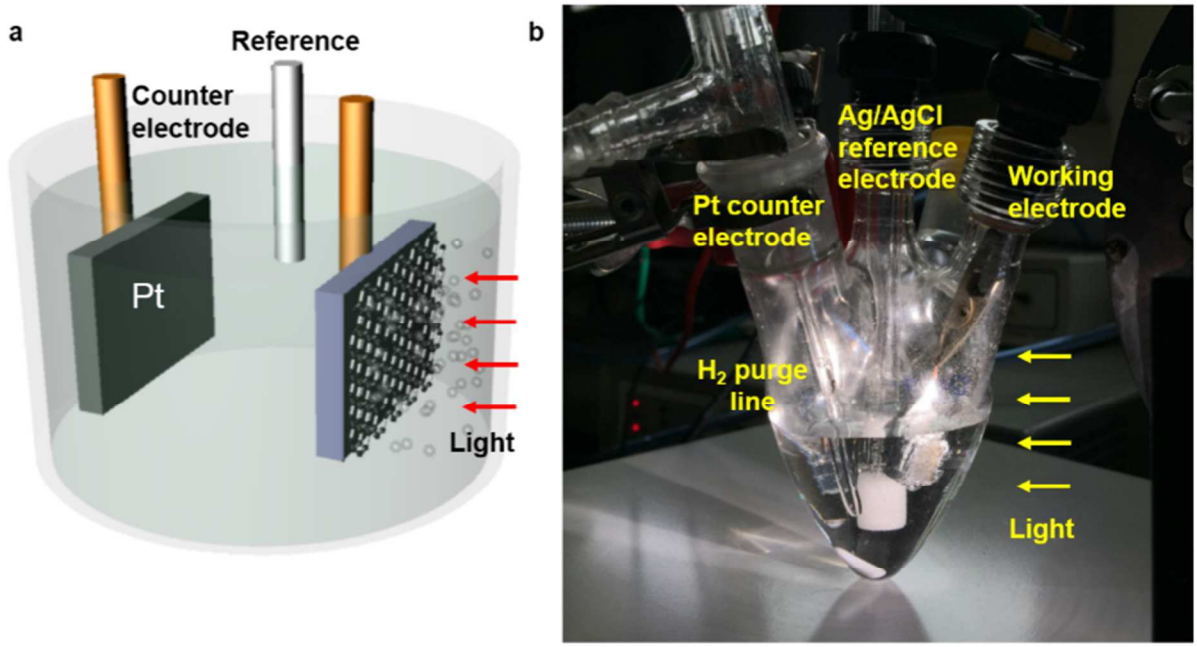

Figure S1. Schematic illustration and photograph images of hydrogen evolution reaction on graphene/Si Photocathode.

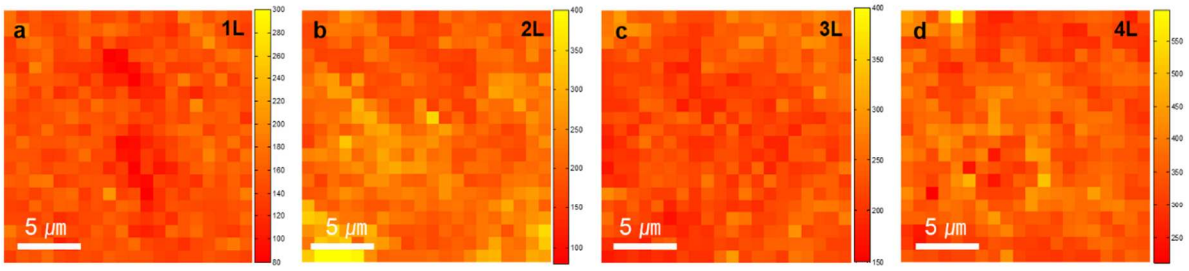

Figure S2. (a-d) Spatially resolved Raman mapping plotted with I(2D) of mono-, bi-, tri- and multilayer graphene, respectively. Scan size: 20 ㎛ x 20 ㎛. Each Raman map shows uniform surface morphology.

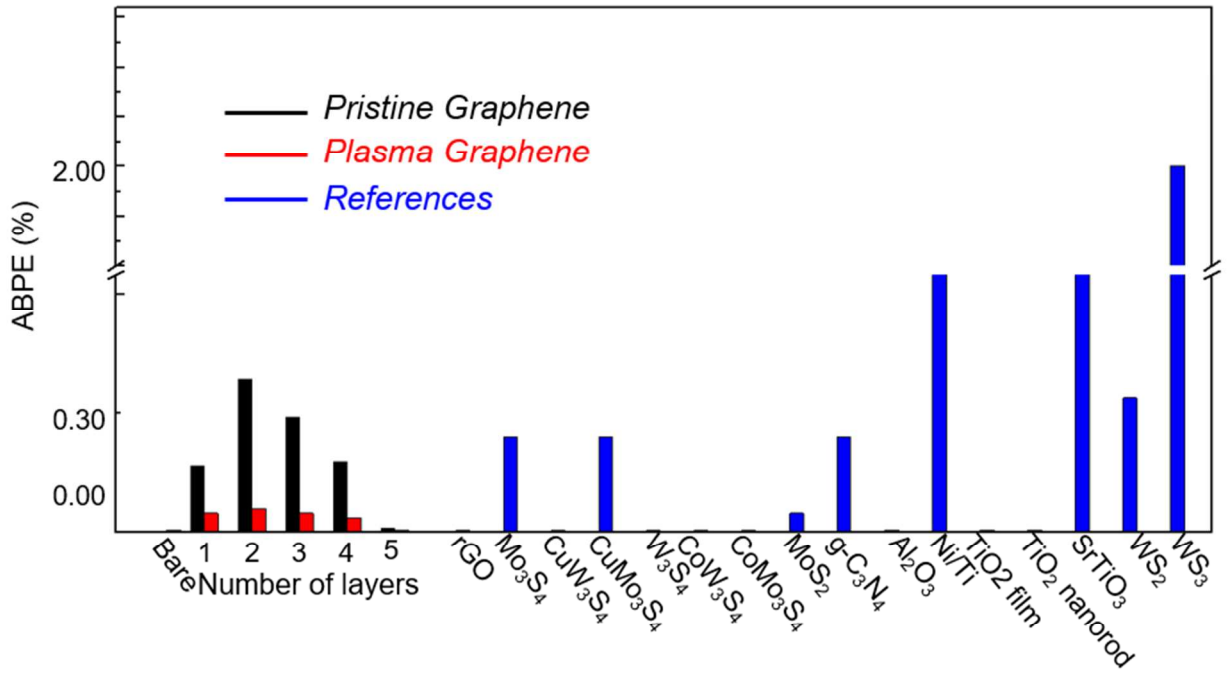

Figure S3. Photoelectrochemical performance of catalysts on p-Si. ABPE indicates applied bias photon-to-current efficiency. 'Bare' indicates the performance of the bare electrode without deposit of the catalyst. Detail information about references can also be shown in Table S1.

Table S1. Summary of experimental data for non-noble metal/metal oxide or carbon-based catalysts on p-Si electrodes.

Electrode	Onset potential [E (V_{RHE} at -1 mA/cm^2]	E (V_{RHE}) at -5 mA/cm^2	E (V_{RHE}) at -10 mA/cm^2	ABPE (%)	References
Bare Si	-0.13	-0.27	-0.35	0.005	This study
Pristine graphene 1-Si	-0.03	-0.09	-0.16	0.04	
Gr 2-Si	0.05	-0.04	-0.11	0.05	
Gr 3-Si	0.04	-0.06	-0.13	0.04	
Gr 4-Si	0.02	-0.10	-0.18	0.03	
Gr 5-Si	-0.10	-0.22	-0.29	0.005	
Plasma Gr 1-Si	0.11	0.01	-0.04	0.14	
Plasma Gr 2-Si	0.15	0.07	0.01	0.32	
Plasma Gr 3-Si	0.15	0.03	-0.06	0.24	
Plasma Gr 4-Si	0.12	0.00	-0.08	0.15	
Plasma Gr 5-Si	-0.03	-0.16	-0.25	0.01	
Bare p-Si	-0.41	-0.55	-0.60	N/A	*Nano Lett.* 2011, **12**, 298
Bare p-Si	-0.35	-0.52	-0.60	N/A	*Energy Environ. Sci.,* 2011,**4**, 1690-1694
Bare p-Si	-0.03	-0.17	N/A (saturated at -9 mA/cm^2)	N/A	*ACS Appl. Mater. Interfaces.* 2013, **5**, 1961
rGO on p-Si	+0.08	-0.05	-0.14	0.005	
Bare	-0.51	-0.64	-0.77	N/A	*Nat. Mater.* 2011, **10**, 434
Mo_3S_4 on p-Si	+0.12	+0.07	-0.01	~0.2	
CuW_3S_4 on p-Si	-0.16	-0.22	-0.29	N/A (~≤0.001)	*J. Photon. Energy* 2012, **2**, 026001
$CuMo_3S_4$ on p-Si	+0.12	+0.06	0.00	~0.2	
W_3S_4 on p-Si	-0.18	-0.25	-0.31	N/A (~≤0.001)	
CoW_3S_4 on p-Si (1st scan)	-0.12	-0.22	-0.3	N/A (~≤0.001)	
$CoMo_3S_4$ on p-Si (1st scan)	-0.02	-0.08	-0.15	N/A (~≤0.001)	
Bare p-Si	-0.50	N/A	N/A	N/A	*Chem. Eur. J.* 2012, **18**,

MoS_2 on Si	-0.06	-0.25	-0.35	0.04	13994
Bare p-Si	-0.25	-0.35	-0.45	N/A	*J. Mater. Chem. A* 2014, **2**, 12697
g-C_3N_4	0	-0.15	-0.25	~0.2	
Bare p-Si	-0.34	-0.47	-0.53	N/A	*Thin Solid Films* 2016, **616**, 550-554
1.4 nm Al_2O_3	-0.21	-0.33	-0.4	N/A (~≤0.001)	
Bare p-Si	-0.05	-0.28	-0.38	N/A	*Nano Res.* 2015, **8**(5), 1577
5 nm Ni/15 nm Ti/p-Si	+0.22	+0.12	0.08	~1.44	
Bare p-Si	-0.7	-0.9	-1.0	N/A	*J. Mater. Chem. A* 2016, **4**, 9477
TiO_2 film/p-Si	-0.4	-0.5	-0.6	N/A	
TiO_2 nanorod/p-Si	-0.05	-0.13	-0.25	N/A (~≤0.002)	
$SrTiO_3$ on p-Si	+0.42	+0.25	+0.01	~1.56	*Nat. Nanotech.* 2015, **10**, 84
WS_2 on p-Si	+0.12	+0.03	-0.04	~0.28	*ACS Appl. Mater. Interfaces.* 2014, **6**, 10408
WS_3 on p-Si	+0.36	+0.27	+0.20	~2	

Values were measured and extrapolated by our group referring to the figures and data from other papers.

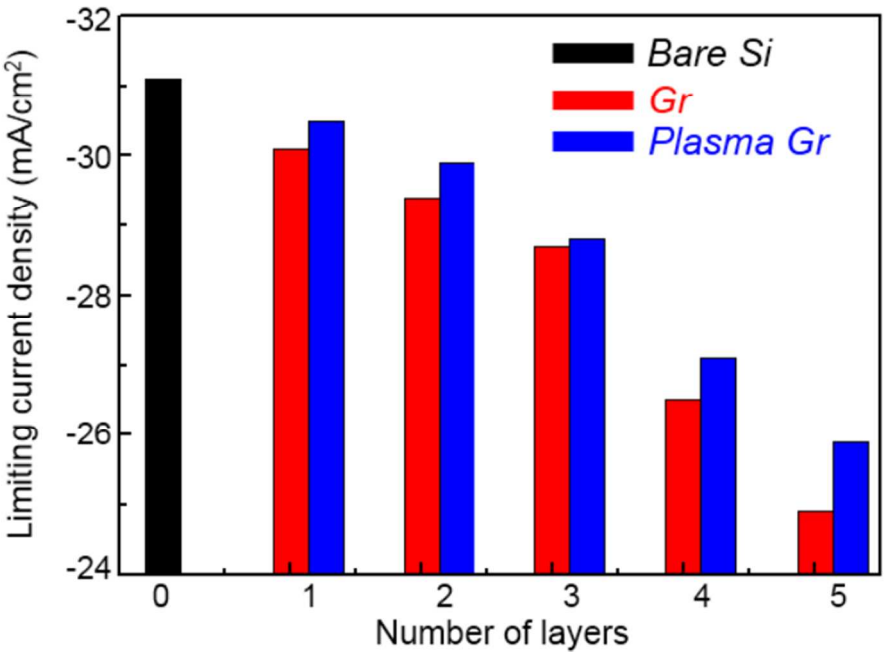

Figure S4. Photoelectrochemical response of graphene on silicon. Saturation current density (Saturation current density) from photocurrent density-potential (J-E) curves of different number of graphene layers on lightly boron-doped planar p-Si electrode.

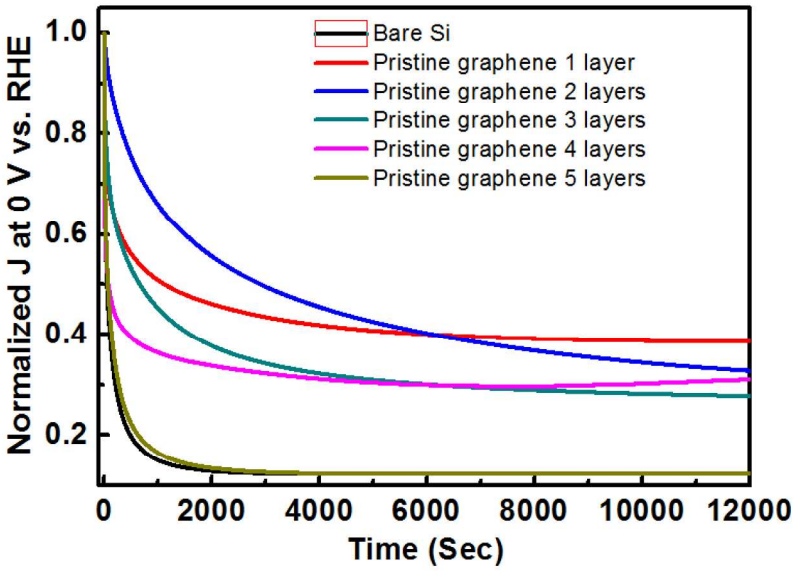

Figure S5. Stability testing of bare Si and graphene layers on Si photocathodes, showing the change in normalized photocurrent density at 0 V vs. RHE of each photoelectrodes as a function of operation time.

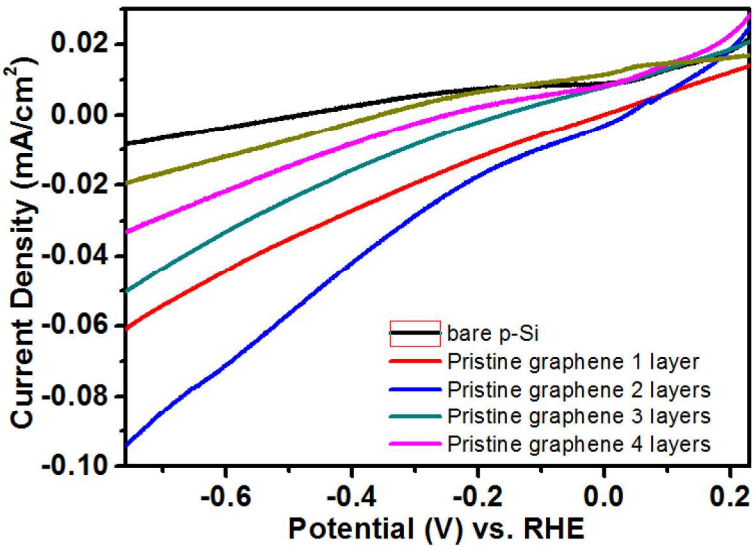

Figure S6. Dark current densities of graphene layers on normal B-doped Si electrodes.

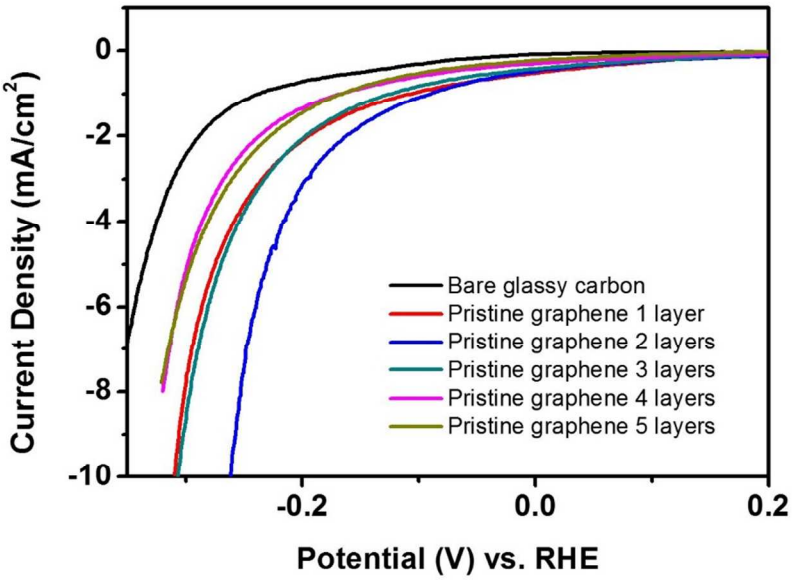

Figure S7. Electrochemical activity of graphene layers on glassy carbon electrode. Cyclivoltammetry (CV) curve of bare glassy carbon, compared to graphene layers on glassy carbon from a rotating disk electrode system. CV data were corrected with iR compensation.

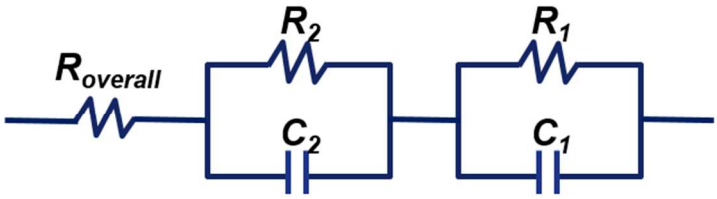

Figure S8. Equivalent circuit to analyze the electrochemical impedance spectroscopy data. $R_{overall}$ is the overall series resistance of the circuit, R_1 is the charge transfer resistance of the double layer at interface between electrode and electrolyte, C_1 is the capacitance phase element of the double layer at interface between electrode and electrolyte, R_2 is the charge transfer resistance of the depletion layer in graphene/Si and C_2 is the capacitance phase element of the depletion layer in graphene/Si.

Table S2. Results obtained from the fitting of the EIS data.

Sample	$R_{overall}$ $(\Omega.cm^2)$	R_2 $(\Omega.cm^2)$	C_2 (F/cm^2)	R_1 $(\Omega.cm^2)$	C_1 (F/cm^2)
Bare Si	*11.65*	*3083*	*2.081E-06*	*-*	*-*
Pristine Gr 1L	*12.76*	*10.51*	*1.49E-06*	*74.39*	*3.439E-06*
Pristine Gr 2L	*11.61*	*8.672*	*2.043E-06*	*33.34*	*7.68E-06*
Pristine Gr 3L	*22.33*	*16.86*	*5.081E-07*	*49.49*	*3.14E-06*
Pristine Gr 4L	*20.32*	*19.906*	*1.54E-06*	*88.26*	*3.918E-06*
Pristine Gr 5L	*24.36*	*17.461*	*2.93E-06*	*218.3*	*4.377E-06*
Plasma Gr 1L	*11.63*	*9.700*	*2.38E-06*	*43.03*	*1.002E-05*
Plasma Gr 2L	*11.74*	*8.588*	*2.057E-06*	*26.11*	*1.16E-05*
Plasma Gr 3L	*17.66*	*12.64*	*1.17E-06*	*40.15*	*6.638E-06*
Plasma Gr 4L	*17.58*	*11.38*	*1.13E-06*	*46.58*	*6.081E-06*
Plasma Gr 5L	*23.71*	*19.372*	*1.360E-06*	*86.74*	*2.44E-06*

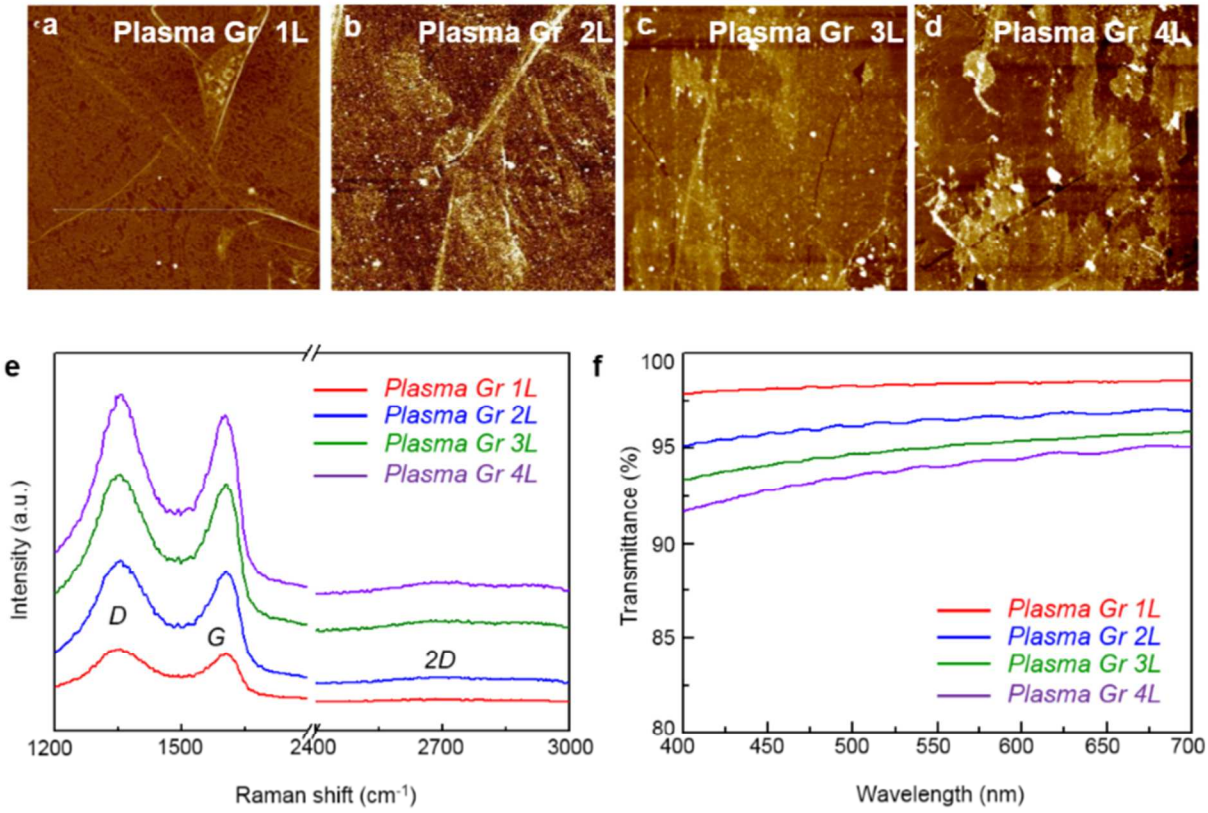

Figure S9. Surface characterization of the different number of plasma-treated graphene layers. a-d, Atomic force microscopy (AFM) images of different number of plasma-treated graphene layers. **e,** Raman spectra of plasma-treated. **f,** Transmittance of plasma-treated graphene specimens on polyethylene terephthalate substrate.

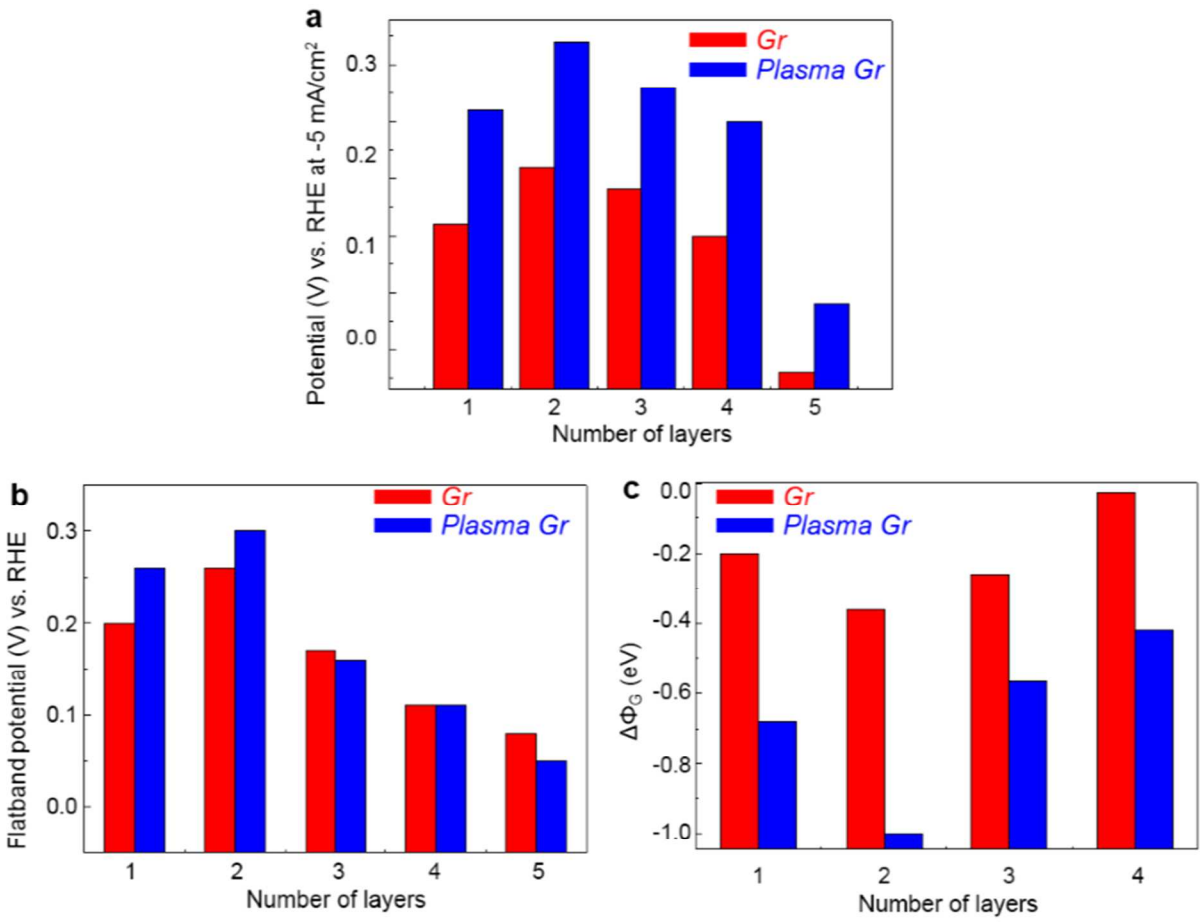

Figure S10. Comparison of electrochemical data between pristine graphene and plasma-treated graphene. a, Potential vs. RHE at -5 mA/cm^2 of different number of graphene layers. **b,** Flatband potential of pristine graphene and plasma-treated graphene. **c,** Work function difference between graphene and the Si.

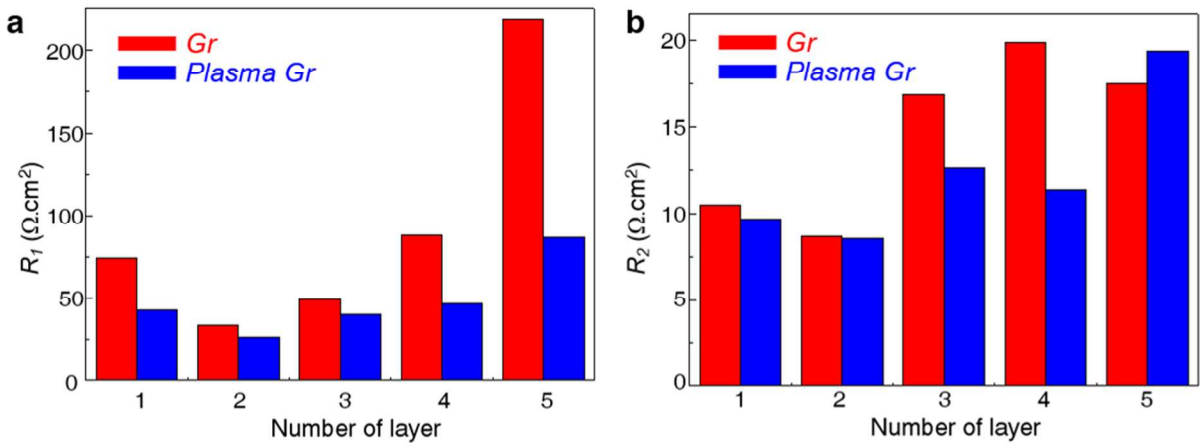

Figure S11. Comparison of electrochemical data between pristine graphene and plasma-treated graphene. Charge transfer resistance of different number of graphene layers. **a**, R_1 is the charge transfer resistance of the electrical double layer at interface between electrode and electrolyte. **b**, R_2 is the charge transfer resistance of the depletion layer in graphene/Si.

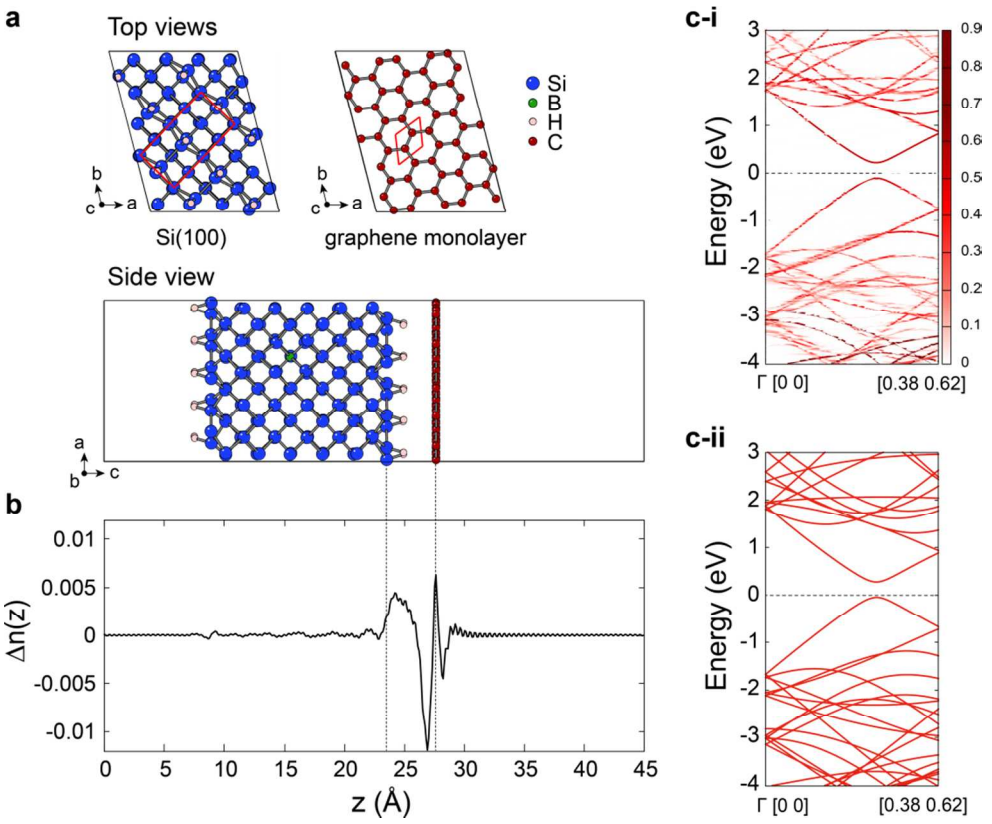

Figure S12. Computational modelling of p-Si/graphene junction. a, Unit cell structure for the modelling within the periodic boundary condition. Red boxes in the top views are unit cells of the reconstructed Si(100) surface and graphene. **b,** xy-plane averaged electron concentration change after junction formation. **c-i (c-ii),** Band structures of graphene monolayer after (before) formation of junction, and the color intensity on c-i shows the weight of C atoms.